ACS central science

Research Article

http://pubs.acs.org/journal/acscii

Shear-Triggered Crystallization and Light Emission of a Thermally Stable Organic Supercooled Liquid

Kyeongwoon Chung,[†] Min Sang Kwon,[‡] Brendan M. Leung,[§] Antek G. Wong-Foy,[∥] Min Su Kim,[¶] Jeongyong Kim,[¶,○] Shuichi Takayama,[†,§,#] Johannes Gierschner,[▽] Adam J. Matzger,[†,∥] and Jinsang Kim*[,†,‡,§,∥,⊥,#]

[†]Macromolecular Science and Engineering, [‡]Department of Materials Science and Engineering, [§]Department of Biomedical Engineering, [∥]Department of Chemistry, [⊥]Department of Chemical Engineering, [#]Biointerfaces Institute, University of Michigan, Ann Arbor, Michigan 48109, United States

[¶]Center for Integrated Nanostructure Physics, Institute for Basic Science (IBS), and [○]Department of Energy Science, Sungkyunkwan University, Suwon 440-746, Republic of Korea

[▽]Madrid Institute for Advanced Studies, IMDEA Nanoscience, Calle Faraday 9, Campus Cantoblanco, 28049 Madrid, Spain

Supporting Information

ABSTRACT: Thermodynamics drive crystalline organic molecules to be crystallized at temperatures below their melting point. Even though molecules can form supercooled liquids by rapid cooling, crystalline organic materials readily undergo a phase transformation to an energetically favorable crystalline phase upon subsequent heat treatment. Opposite to this general observation, here, we report molecular design of thermally stable supercooled liquid of diketopyrrolopyrrole (DPP) derivatives and their intriguing shear-triggered crystallization with dramatic optical property changes. Molten DPP8, one of the DPP derivatives, remains as stable supercooled liquid without crystallization through subsequent thermal cycles. More interestingly, under shear conditions, this supercooled liquid DPP8 transforms to its crystal phase accompanied by a 25-fold increase in photoluminescence (PL) quantum efficiency and a color change. By systematic investigation on supercooled liquid formation of crystalline DPP derivatives and their correlation with chemical structures, we reveal that the origin of this thermally stable supercooled liquid is a subtle force balance between aromatic interactions among the core units and van der Waals interactions among the aliphatic side chains acting in opposite directions. Moreover, by applying shear force to a supercooled liquid DPP8 film at different temperatures, we demonstrated direct writing of fluorescent patterns and propagating fluorescence amplification, respectively. Shear-triggered crystallization of DPP8 is further achieved even by living cell attachment and spreading, demonstrating the high sensitivity of the shear-triggered crystallization which is about 6 orders of magnitude more sensitive than typical mechanochromism observed in organic materials.

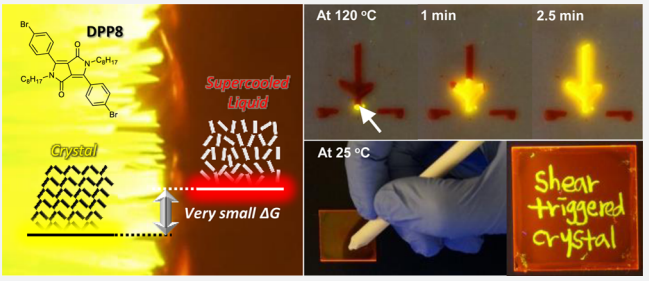

INTRODUCTION

When molten organic crystalline materials are cooled below their melting temperature (T_m), exothermic crystallization is usually observed and the molecules revert to the energetically favorable crystalline phase. Even though some crystalline organic materials can stay in a supercooled liquid state (above glass transition temperature, T_g) or a glass state (below T_g) upon rapid cooling, these materials crystallize upon subsequent heating.[1−4] Only a few crystalline organic molecules exhibit thermally stable supercooled liquid without crystallization despite their energetically more favorable crystalline phase and sufficient mobility of the molecule above T_g.[5−8] In fact, the thermal stability of amorphous organic materials including supercooled liquids and glasses is a subject of considerable commercial importance. For example, conjugated organic glasses without good thermal stability can derogate the reliability of organic electronic devices due to device failure by crystallization during the operation.[9−11] In the field of drug delivery, pharmaceutical organic glasses have been widely studied due to their advantageous solubility, bioavailability, and consistent efficacy.[7,12] However, unlike those widely researched and exploited organic glasses, organic supercooled liquids have been investigated mainly in theoretical aspects such as the glass transition phenomenon and structural relaxation dynamics.[2,13−16]

Diketopyrrolopyrrole (DPP) derivatives have been widely used as high performance pigments[17] as well as one of the frequently used building blocks for conjugated polymers in electronic applications[18,19] due to strong intermolecular

Received: March 9, 2015
Published: May 13, 2015

DOI: 10.1021/acscentsci.5b00091
ACS Cent. Sci. 2015, 1, 94−102

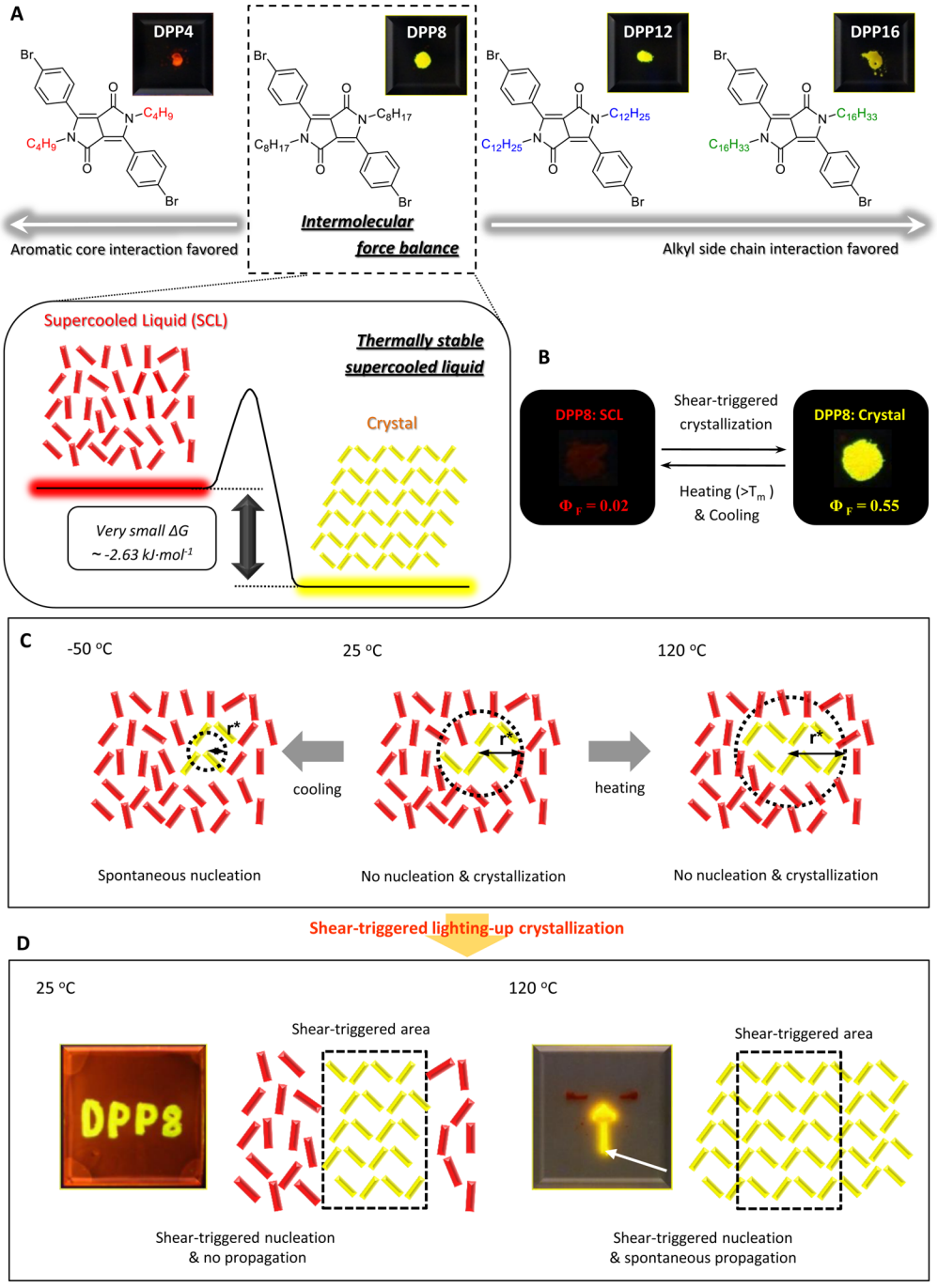

Figure 1. Schematic illustration of the thermally stable supercooled liquid and shear-triggered lighting-up crystallization of DPP8. (A) Chemical structure of DPP8 and its derivatives. A subtle force balance between two different intermolecular interactions acting in opposite directions makes DPP8 exhibit small ΔG between supercooled liquid and crystalline solid phases, resulting in intriguing thermally stable supercooled liquid. Fluorescence images are from crystalline solids of the derivatives. (B) Reversible phase transformation with large optical property change between the two forms by means of independent stimuli. (C) Nucleation is restricted in DPP8 supercooled liquid due to an unattainable yet required large critical radius (r^*), which results from small ΔG between two phases, at 25 and 120 °C. However, when molten DPP8 was cooled to −50 °C, subsequent heating developed crystallization. (D) Shear-triggered lighting-up crystallization of DPP8. Photographs (A, B, and D) were taken under 365 nm UV light.

interactions between the DPP units. During the investigation on DPP derivatives as a monomeric unit of conjugated polymers, we observed that a DPP molecule, DPP8, formed both a crystalline solid and a stable supercooled liquid at room temperature. The stable supercooled liquid DPP8 did not transform back to crystalline solid even under subsequent heating and cooling cycles. It is an intriguing question what the origin of thermally stable supercooled liquid is and what chemical features make organic crystalline materials form an extraordinarily stable supercooled liquid. We examined the mechanism and molecular features allowing the stable supercooled liquid formation. For a systematic investigation, a series of DPP derivatives with altered alkyl chain length, DPP4, DPP8, DPP12, and DPP16, are synthesized and characterized

DOI: 10.1021/acscentsci.5b00091
ACS Cent. Sci. 2015, 1, 94−102

in terms of supercooled liquid formation and their thermal stability (Figure 1A).

Interestingly, the stable supercooled liquid DPP8 crystallizes by shear force accompanied by dramatic optical property changes. Even though the role of shear stress in crystallization has been investigated both experimentally and theoretically, the relationship is still not conclusive; several studies report shear-induced ordering with enhancing nucleation rate, while others report suppression of crystallization by shear force.[20−26] Macromolecules with a large aspect ratio such as isotactic polypropylene and polystyrene can be crystallized by shear force due to chain alignment.[27−29] However, the shear-triggered crystallization of DPP8 with a remarkable optical property change is an intriguing phenomenon observed from organic small molecules.

In a phenomenological view, shear-triggered lighting-up crystallization is quite similar to the mechanochromism of organic compounds.[30−34] Mechanochromic organic compounds show color and/or fluorescence change when external forces such as pressure and shear are applied. However, while mechanochromism is based on polymorphism or on an order-to-disorder transformation (i.e., breaking the crystalline structure toward amorphous or disrupting secondary bonding such as hydrogen bonding) by applied mechanical force, the shear-triggered crystallization reported here is a distinctive disorder-to-order transition.

Our investigation revealed that DPP8 has the highest thermal stability of supercooled liquid among the derivatives, and the thermal stability is ascribed to small Gibbs free energy difference between supercooled liquid and crystalline solid that is originated from a subtle force balance between aromatic interactions among the core units and van der Waals interactions among the aliphatic side chains working in opposite directions (Figure 1A). Furthermore, we demonstrate direct writing of fluorescent patterns and propagating fluorescence amplification, respectively, by applying shear to a supercooled liquid DPP8 film at different temperatures. A threshold shear rate of 0.03 s^{-1} and the corresponding shear stress of 0.90 kPa for shear-triggered crystallization were measured by rheometry, which is a million times smaller than the typically required stress range for mechanochromism observed in organic materials (1 GPa).[35,36] The high sensitivity of the shear-triggered crystallization was further confirmed by crystallization of a supercooled DPP8 film even by living cell attachment and spreading.

RESULTS AND DISCUSSION

We designed and synthesized DPP8 as a monomeric unit of a series of conjugated polymers. During the characterization of this compound, we observed an interesting phenomenon. While crystalline DPP8 powder, purified by recrystallization, melts at 134 °C as seen in the differential scanning calorimetry (DSC) trace in Figure 2A, subsequent cooling of the molten DPP8 results in a supercooled liquid phase stable down to 25 °C, equivalent to more than a range of 100 °C below the melting temperature. The supercooled liquid phase persists during the second and third DSC cycles without showing any crystallization peaks. No crystallization is observed even at a very slow cooling rate of 0.2 °C·min^{-1} (Figure 2A).

In order to investigate the chemical features that make DPP8 so special in forming such thermally stable supercooled liquid, we synthesized three more DPP derivatives having butyl (DPP4), dodecyl (DPP12), and hexadecyl side chains (DPP16)

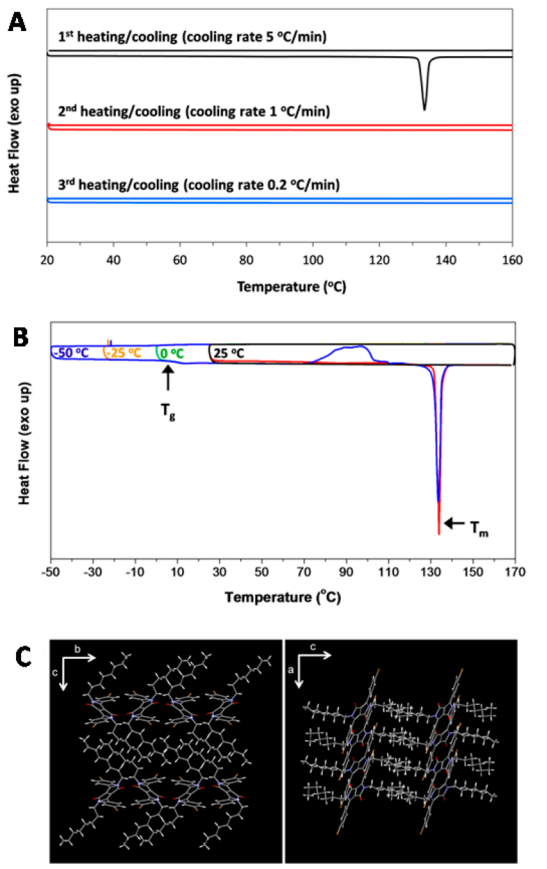

Figure 2. Thermal properties and single crystal structure of DPP8. (A) DSC trace at different cooling rates (heating rate: 10 °C·min^{-1}). (B) DSC trace with different cooling temperatures (scan rate: heating 10 °C·min^{-1}, cooling 5 °C·min^{-1}). A glass transition (T_g) was observed at 5 °C. Only after cooling down to −50 °C, subsequent heating developed crystallization begins at 72 °C followed by melting at 134 °C. (C) Single crystal structure of DPP8. Weakly coupled DPP cores and lamellar-type packing of the octyl side chains are observed.

(Figure 1A). The DPP core unit without alkyl chains is hardly soluble in organic solvents due to strong intermolecular interactions and consequently produces red fluorescent emission with negligible quantum yield due to the well-known concentration induced self-quenching. However, the introduction of the octyl chains in DPP8 makes DPP8 form weakly coupled aromatic DPP cores together with lamellar-type octyl chain packing as evident from the X-ray crystal structure (Figure 2C and Table S1). Strong hydrogen bonding, $\pi-\pi$ interaction, or halogen bonding is not observed.

Different from DPP8, molten DPP4 crystallizes upon cooling (Figure 3A). The DPP4 crystal shows red fluorescence, which is largely red-shifted from the greenish yellow emission of the DPP8 crystal (Figure 1A and Figure 3B), and is ascribed to closely packed aromatic core units just like the unsubstituted DPP core unit. The DPP4 crystal shows strikingly different powder XRD pattern and single crystal structure compared to DPP8 (Figure 3C and Figure S1); different from the weakly coupled DPP8 aromatic cores, the DPP4 cores are closely packed with a distance of ca. 3.5 Å (Figure S1). DPP12 and DPP16 on the other hand show identical PL emission (Figure 1A and Figure 3B) and similar powder XRD patterns as DPP8 (Figure 3C), implying similarly weakly coupled aromatic cores and lamellar-type packing of the side chains. The alkyl chain

DOI: 10.1021/acscentsci.5b00091
ACS Cent. Sci. 2015, 1, 94−102

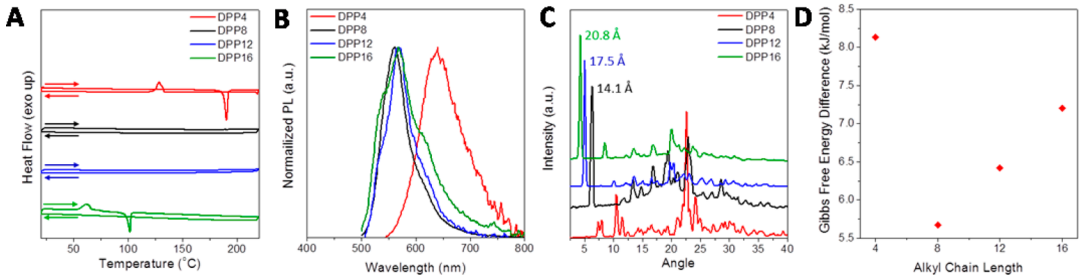

Figure 3. Effects of molecular design on thermal, optical, molecular packing properties, and ΔG characteristics. (A) DSC trace (2nd cycle) of DPP derivatives (scan rate 10 °C·min $^{-1}$). (B) Normalized PL of shear-triggered (DPP8 and DPP12) and thermally driven (DPP4 and DPP16) crystals. (C) Powder XRD traces. DPP8, -12, and -16 have similar lamellar packing patterns in contrast to the drastically different diffraction pattern of DPP4. (D) ΔG between the crystalline solid and supercooled liquid phases of DPP derivatives (from the Hoffman equation, at 26 °C).

length represented in the lamellar distance increases linearly from n = 8 to 12 to 16 in steps of ca. 3.4 Å as calculated from the sharp peaks at ca. 5° in the powder XRD trace (Figure 3C). Even though the packing seems to be similar to that of DPP8, the thermal stability of the supercooled liquid of DPP12 and DPP16 is not the same as that of DPP8. While DPP8 did not show crystallization upon subsequent heating until the cooling temperature reached −50 °C (Figure 2B), DPP12 showed crystallization beginning at 57 °C and melting at 108 °C upon subsequent heating after it was cooled down to 0 °C (Figure S2). Moreover, DPP16 needed to be cooled to only 20 °C in order to show a broad crystallization peak followed by melting at 102 °C upon subsequent heating (Figure 3A).

Apparently, the different alkyl chain length of the DPP derivatives triggers a distinctive difference in the thermal stability of their supercooled liquids: DPP8 is most stable among the derivatives, and when the alkyl chain is shorter (DPP4) or longer (DPP12 and -16) than octyl, the thermal stability of the supercooled liquid diminishes. From these results, we attribute the origin of the thermally stable supercooled liquid of DPP8 to a delicate force balance between the aromatic interactions and aliphatic van der Waals forces acting in opposite directions (Figure 1A). If the alkyl chain is short (DPP4), strong interactions among the DPP cores induce crystallization upon cooling of the melt because the van der Waals interactions among the short alkyl chain cannot provide strong enough force to balance against the interactions. On the contrary, as the alkyl chain gets longer (DPP12 and DPP16), the van der Waals interactions among the lamellar packed alkyl side chains become stronger than the interactions between the weakly coupled DPP cores, resulting in less thermally stable supercooled liquid. Then, how does this delicate force balance built in DPP8 suppress the crystallization of DPP8?

In order to achieve a thermally stable supercooled liquid, nucleation in the supercooled state should be forbidden. Otherwise, even though molten organic crystalline materials may remain as supercooled liquid at a reduced temperature due to the restricted molecular mobility and the ensuing retarded crystal growth, they will eventually crystallize upon subsequent heating. In homogeneous nucleation theory, the Gibbs free energy of nucleation in a supercooled liquid is expressed as the sum of the energy gain (driving force) by generating an energetically more favorable crystalline nucleus and the energy loss by producing the interface, driven by surface tension (see Supporting Information, Homogeneous Nucleation Theory). If ΔG between supercooled liquid and crystalline solid is very small, the critical radius of nucleation (r*), the minimum size of nucleus which can continue growing spontaneously, largely increases so that nucleation is suppressed, promoting kinetically entrapped supercooled liquid formation. In other words, a small ΔG between the supercooled liquid and crystalline solid states results in unattainable yet required large critical radius r* so as to restrict nucleation. We hypothesize that the supercooled liquid DPP8 is thermally stable because nucleation is forbidden over such a large supercooling temperature range (over 100 °C) due to very small ΔG between the supercooled liquid and the crystalline solid, which is originated from the subtle force balance between the two different intermolecular interactions acting in opposite directions as schematically illustrated in Figure 1, panels A and C. In other word, DPP8 is expected to have a particularly small value of ΔG.

The fact that nucleation is forbidden in the supercooled liquid DPP8 was proven by means of a seeding test with the crystalline powder (Movie S1 and Movie S2). When DPP8 crystalline powder was dropped onto the supercooled liquid at 120 °C, the crystallites served as stable nuclei so that crystallization propagated through the entire area of the connected supercooled liquid due to the sufficient molecular mobility. In contrast, the adjacent yet disconnected supercooled liquid domain did not show crystallization due to the absence of nuclei. Seeding at 25 °C on the other hand did not induce spontaneous propagation of crystallization due to limited molecular mobility. However, when the temperature was increased to ∼70 °C, crystallization began to propagate, which means that in pristine supercooled liquid state nuclei are absent even at 25 °C. Taken together with the thermal cycling experiments, these findings demonstrate that nucleation is the limiting step in DPP8 crystallization. If the required large critical radius r* which results from small ΔG between two phases is responsible for the absent crystallization as suggested (Figure 1C), there should be a threshold temperature at which the required critical radius r* can be extremely small due to large supercooling. Indeed, while the supercooled liquid was stable down to −25 °C, cooling to −50 °C and subsequent heating induced crystallization (Figure 2B).[37] When the crystallized DPP8 was melted again and cooled to room temperature, no crystallization was observed upon subsequent heating, implying that crystallization of DPP8 is independent of thermal history.

Now, the question is whether ΔG between the supercooled liquid and the crystalline solid is indeed small. The single crystal structure of DPP8 does not show close packing but only weakly coupled aromatic DPP cores and lamellar-type octyl chain packing (Figure 2C). ΔG between the two phases of DPP8 was estimated to be −2.63 kJ·mol^{-1} (−0.63 kcal·mol^{-1}) at 26 °C by means of relative solubility measurements (Figure S3).[38] We

DOI: 10.1021/acscentsci.5b00091
ACS Cent. Sci. 2015, 1, 94−102

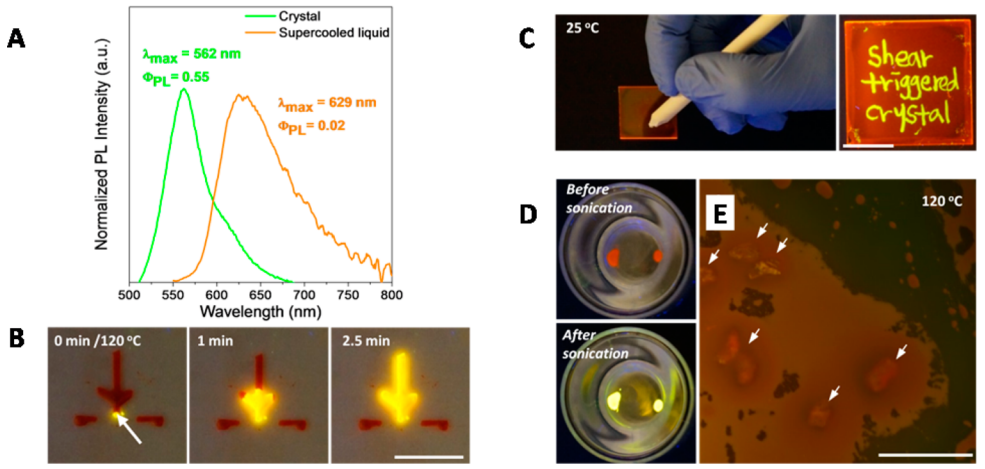

Figure 4. Different optical property of the two phases and shear-triggered lighting-up crystallization of DPP8: role of shear and dual mode crystallization. (A) Normalized fluorescence emission spectra and quantum yields of DPP8 crystal and supercooled liquid at room temperature. (B) Shear at the tip (white arrow) of the tree-shape supercooled DPP8 pattern triggered crystallization and propagation through the entire tree pattern at 120 °C. However, the two disconnected horizontal lines stayed at the supercooled liquid state (scale bar: 1 cm). (C) Direct writing of fluorescent patterns at 25 °C. The only shear-applied area turned into greenish yellow crystals (scale bar: 1 cm). (D) Supercooled liquid DPP8 before sonication and after sonication followed by heating to 120 °C. Sonic wave was applied as a source of molecular agitation. (E) In order to study the effects of intentionally introduced heterogeneous nucleation sites, sea sands (white arrows) were mixed with DPP8 melt followed by cooling to 25 °C and subsequent heating to 120 °C. Fluorescence image under optical microscope was taken after 5 min at 120 °C (scale bar: 0.5 mm). Photographs (B, C, and D) were taken under 365 nm UV light.

also used the Hoffman equation to calculate $\Delta G = -5.67$ kJ·mol^{-1} (-1.35 kcal·mol^{-1}) at 26 °C (Figure S3).[39] ΔG can also be estimated from a thermodynamic cycle (Hess's law) utilizing $\Delta G = \Delta H - T\Delta S$, where ΔH and ΔS can be deduced from heat capacity via Kirchhoff's law, giving $\Delta G = -6.24$ kJ·mol^{-1} (-1.49 kcal·mol^{-1}) at 26 °C from this third method (Figure S3). Hence, the three methods consistently gave a small ΔG value (2.63–6.24 kJ·mol^{-1}), which is comparable to the ΔG between polymorphs[38] and is even much smaller than 50.21 kJ·mol^{-1} (12 kcal·mol^{-1}) of the ΔG between *cis*- and *trans*-azobenzene, a well-known photoisomerizable compound.[40] Therefore, the thermally stable supercooled liquid state of DPP8 is due to the unattainable yet required large critical radius r^* originating from a small ΔG between the supercooled liquid and crystalline solid states.

The calculated ΔG values between supercooled liquid and crystalline solid clearly represent the trend of thermal stability of supercooled liquid of the derivatives (Figure 3D). ΔG of the derivatives were calculated from the Hoffman equation.[39] DPP4 with the highest ΔG value from Hoffman equation shows crystallization upon cooling of melt because the crystal is much more stable than the supercooled liquid state (Figure 3A). DPP16 shows crystallization upon subsequent heating after cooling to 25 °C. DPP12 shows crystallization upon subsequent heating after cooling to 0 °C. DPP8, with the lowest ΔG, exhibits the most stable supercooled liquid compared to the rest of derivatives, which again implies that the small ΔG of DPP8 provides the smallest driving force for crystallization, whereas larger van der Waals interactions between molecules (DDP12 and DDP16) or stronger core interactions (DPP4) increase the driving force. Therefore, the subtle force balance between the aliphatic side chains and the aromatic core of DPP8 is the key feature to make its ΔG small enough to suppress crystallization and ensuring a thermally stable supercooled liquid.[41]

Although the Gibbs free energy difference between supercooled liquid and crystalline solid of DPP8 is very small, the differences in the optical properties are dramatic (Figure 4A). The PL emission of the crystal is bright greenish yellow with emission at λ_{max} = 562 nm and a PL quantum yield of Φ_{PL} = 0.55 in contrast to the dim orange-red emission of the supercooled liquid having λ_{max} = 629 nm and Φ_{PL} = 0.02 (see Supporting Information, Photophysical Properties of DPP8).

Interestingly, upon applying shear force, the dim orange-red fluorescent supercooled liquid transforms to bright greenish yellow fluorescent crystals (Figure 4B,C, Figure 1B,D). We hypothesized that the shear force might induce rearrangement and density fluctuation of DPP8 molecules and thereby help embryos surpass the critical radius of nucleation to become active nuclei.[15] To verify the proposed role of shear force in the shear-triggered crystallization of DPP, we investigated the effect of molecular agitation on the crystallization of supercooled liquid DPP8. In this experiment, sonic wave was applied as an external energy source to induce rearrangement and density fluctuation of DPP8 molecules through simple agitation of DPP8 molecules in the supercooled liquid. Applied sonic wave helps nucleation in supercooled liquid DPP8 and develops crystallization upon subsequent heating as shown in Figure 4D (also see Figure S4), supporting the hypothesis that rearrangement and density fluctuation of DPP8 by external energy, such as shear force and sonic wave, can stimulate nucleation.

The role of shearing in the shear-triggered crystallization was further verified by adding sea sand, as a heterogeneous nucleation site, to supercooled liquid DPP8. It has been well-known that the nucleation is promoted when heterogeneous nucleation sites, such as rough or scratched surface, are provided in the system.[42−44] Sea sand was mixed with molten DPP8, and the mixture was cooled to room temperature followed by subsequent heating to 120 °C. Even though DPP8 molecules have enough mobility at this temperature and even in the presence of interfaces provided by sea sand, no crystallization was observed (Figure 4E). Similarly, no crystallization was observed even when hydrophobic particles, including rubber powders from the same eraser used for the

DOI: 10.1021/acscentsci.5b00091
ACS Cent. Sci. 2015, 1, 94−102

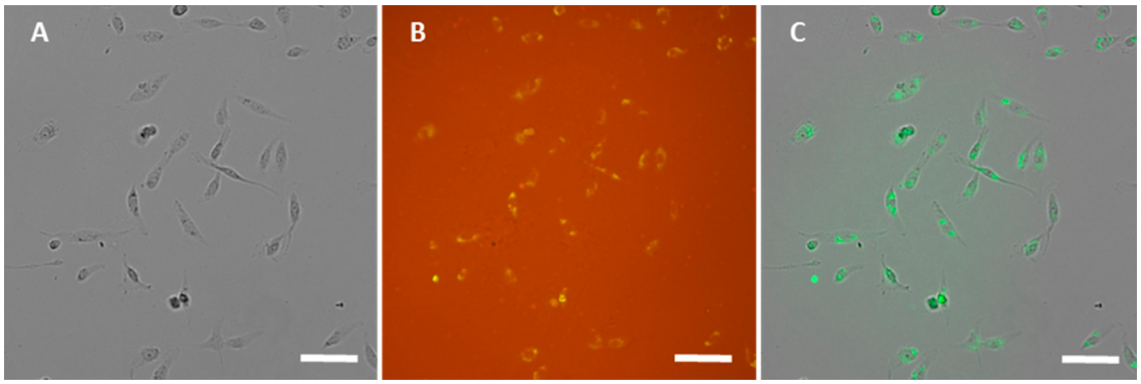

Figure 5. Shear-triggered crystallization by living cell attachment. (A) Bright field image and (B) fluorescence image of HS-5 cells on the supercooled liquid DPP8 film after 2-day incubation. The background orange fluorescence in panel B originated from the supercooled liquid phase of DPP8, and traction force produced by cell focal adhesion complex on a supercooled liquid DPP8 film triggered crystallization resulting in greenish yellow fluorescence in panel B. (C) In order to visualize the alignment of cell positions relative to the fluorescent signals from the induced DPP8 crystals by cell adhesion, the greenish yellow crystalline fluorescent signals were isolated from panel B and labeled as green, and overlaid with panel A (scale bar: 100 μm).

fluorescence pattern writing on a DPP8 supercooled liquid film (see below and Figure 4C), were added as foreign interfaces to induce heterogeneous nucleation (Figure S5). Therefore, heterogeneous nucleation possibility by physical contact with the shearing tool is unlikely in the shear-triggered crystallization of DPP8. It should be noted that, under heterogeneous nucleation conditions, the provided interface promotes stable nucleus formation by reducing the surface energy term (second term of eq 1 in the Supporting Information). In supercooled liquid DPP8, however, crystallization is absent even when such a rough hydrophobic interface is provided. Therefore, it is highly plausible to attribute the restricted nucleation to small ΔG between the two phases, resulting in a small driving force for crystallization (first term in eq 1 in Supporting Information) as suggested.

Consequently, shear force is acting as a trigger for crystallization via molecular agitation in this system. Both crystal structure and PL features of the shear-triggered crystal essentially resemble the original crystal powder of DPP8 (Figure S6). Because the crystal growth rate varies at different temperatures, the shear-triggered lighting-up crystallization propagates in a very different way depending on temperature. At 120 °C, crystallization propagated through the entire connected area of supercooled liquid and gave corresponding large fluorescence amplification even though the shear was applied only at the tip of the supercooled liquid domain (Figure 4B, Movie S3 and Movie S4). The shear-triggered crystallization is observed as well for the supercooled highly viscous liquid DPP8 film at 25 °C. However, the propagation of crystallization is restricted due to the limited molecular mobility at 25 °C, and thus fluorescent patterning by direct writing on the supercooled liquid DPP8 film was accomplished. In this case, only the shear-applied area showed bright greenish yellow emission (Figure 4C). In addition, the transformation between the supercooled liquid and the crystalline solid is completely reversible. Shear-triggered crystals can be transformed to supercooled liquid by simple heating over its T_m and subsequent cooling. Upon heating, the crystalline part disappears with vanishing bright fluorescence in a few seconds (Movie S5), and the transformed supercooled liquid is crystallized again by applying shear force.

Unlike the mechanochromism of organic materials, this shear-triggered crystallization is a disorder-to-order transition. In this system, the applied shear force does not change an energetically favorable structure to another structure but triggers crystallization which propagates spontaneously afterward. To test the sensitivity of the shear-triggered crystallization, we used living cells as a shear force source. When cells are seeded on a substrate, they spread and establish focal contacts on the substrate.[45] These focal adhesions transmit intracellular tension generated by the actin cytoskeleton into traction force against extracellular substrate.[46] In the case of fibroblast cells, such as NIH-3T3 embryonic fibroblast and dermal fibroblast, average cell traction force (CTF) per unit area has been reported in the range of 0.1−0.3 kPa over compliant polyacrylamide gel,[47] but local CTF per unit area can be in the 1−5 kPa range.[46,48,49] In this experiment, we used HS-5 bone marrow fibroblast cells, which belong to the larger family of stromal fibroblast, seeded on DPP8 to induce local crystallization. After 2-day incubation, the HS-5 cells attached and spread over a supercooled liquid DPP8 film (Figure 5A) and produced clear greenish yellow fluorescent marks against the orange fluorescent supercooled liquid area without cells (Figure 5B). In order to visualize the alignment of cell positions relative to the greenish yellow fluorescent signals from the induced DPP8 crystals by cell adhesion, bright field image (Figure 5A) and fluorescence image (Figure 5B) were processed and merged in Figure 5C. The greenish yellow crystalline fluorescent signals were isolated from Figure 5B and labeled as green, followed by merging with gray bright field image, Figure 5A. In the resulting Figure 5C, the location of crystalline fluorescence perfectly matches within the cell boundary of HS-5 cells, which demonstrates that the shear-triggered crystallization of supercooled liquid DPP8 is sensitive enough to detect cell attachment and cell contraction.[50]

In order to provide more quantitative information, we additionally conducted analysis on the threshold shear rate and shear stress of the shear-triggered crystallization by using a rheometer. In this experiment, the supercooled liquid DPP8 sample was sandwiched between two parallel plates, and the nucleation in the supercooled liquid DPP8 was examined under different applied shear rates, from 0.001 to 10 s^{-1} (shear stress from 0.03 to 273.84 kPa), at ca. 29 °C (Figure 6A,B). Under each shear rate condition, nucleation was confirmed by observing crystallization propagation upon subsequent heating to 100 °C immediately after the shearing process. As presented

DOI: 10.1021/acscentsci.5b00091
ACS Cent. Sci. 2015, 1, 94−102

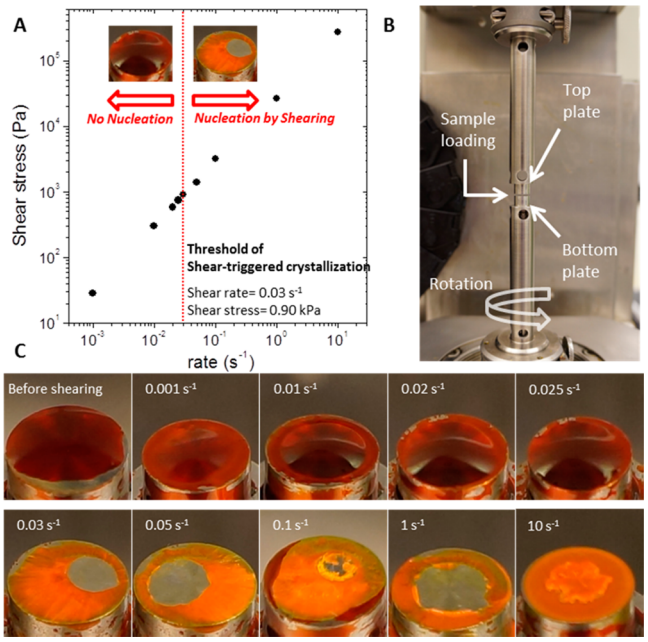

Figure 6. Sensitivity of the shear-triggered crystallization. (A) Applied shear rate and stress on the supercooled liquid DPP8 under a rheometer (ca. 29 °C). Nucleation by shearing was first observed at the applied shear rate of 0.03 s^{-1} (shear stress of 0.90 kPa). (B) Experimental rheometer setup to quantitatively analyze the threshold shear rate to trigger nucleation. (C) Images of DPP8 sample on the bottom plate after applying each shear rate followed by heating to 100 °C. No crystallization was observed up to the shear rate of 0.025 s^{-1} (shear stress 0.74 kPa). At the shear rate 0.03 s^{-1} and above, crystallization was clearly observed due to crystal nucleation induced by the applied shearing. Photographs (B and C) were taken under room light.

in Figure 6C, the shear rates up to 0.025 s^{-1} (shear stresses up to 0.74 kPa) do not induce any crystallization but retain the thermally stable supercooled liquid phase. The nucleation in the DPP8 supercooled liquid phase is first confirmed at the shear rate of 0.03 s^{-1} (shear stress of 0.90 kPa) by massive crystallization propagation upon subsequent heating. In the higher shear rate range (0.05−10 s^{-1}), shear-triggered crystallization is similarly observed. We note that this threshold shear stress value (0.90 kPa) is comparable to the fibroblast cells' traction force per unit area (1−5 kPa), and implies that the shear-triggered crystallization is about 6 orders of magnitude more sensitive than the mechanochromism observed in organic materials; in the literature these organic materials show color and/or fluorescence change at around 1 GPa.[35,36]

CONCLUSION

In summary, we have presented that a subtle force balance between core interactions and side chain interactions acting in opposite directions can be a molecular design strategy to achieve a thermally stable supercooled liquid of conjugated organic molecules. Applying shear force on the thermally stable supercooled liquid can trigger spontaneous crystallization with large optical property changes. We demonstrated these findings by investigating rationally designed DPP derivatives. A crystalline organic compound, DPP8, formed a thermally stable supercooled liquid state even over a 100 °C supercooling range because of a small Gibbs free energy difference, ΔG, between its supercooled liquid and the crystalline solid states. Our investigation shows that this phenomenon is derived from a subtle force balance between aromatic core interactions and van der Waals interactions among the aliphatic side chains. The supercooled liquid DPP8 was readily transformed to its original crystal structure by means of applied shear force accompanied by 25-times fluorescence enhancement and color change. By adjusting the crystal growth rate through temperature control, we demonstrated shear-triggered fluorescent fine patterning at room temperature and propagating fluorescence amplification at 120 °C, respectively, in a completely reversible manner, which can be potentially adapted to a novel optical storage system. The lighting-up crystallization of the supercooled liquid DPP8 film by living cell attachment and spreading demonstrates the possibility of applying the phenomenon to fluorescence sensor development having sensitive turn-on signaling.

METHODS

Details on methods, materials, and synthesis are available in the Supporting Information.

ASSOCIATED CONTENT

Supporting Information

The following files are available free of charge on the ACS Publications website at DOI: 10.1021/acscentsci.5b00091.

Detailed experimental procedures, materials and synthesis (PDF)

Seeding test at 120 °C (MPG)

Seeding test at 25 °C followed by heating to 100 °C (MPG)

Shear-triggered crystallization at 120 °C (MPG)

Crystallization propagation at 120 °C (MPG)

Transformation from crystals to supercooled liquid at 150 °C (MPG)

X-ray data for $C_{34}H_{42}Br_2N_2O_2$ (CIF)

X-ray data for $C_{26}H_{26}Br_2N_2O_2$ (CIF)

AUTHOR INFORMATION

Corresponding Author

*E-mail: jinsang@umich.edu.

Notes

The authors declare no competing financial interest.

ACKNOWLEDGMENTS

The authors thank Dr. J. W. Kampf for assistance on single crystal structure analysis, Dr. S. Seo for assistance on powder XRD characterization, and P. Desai and Dr. R. G. Larson for assistance on the rheometer experiment. This work was supported as part of the Center for Solar and Thermal Energy Conversion, and Energy Frontier Research Center funded by the U.S. Department of Energy (DoE), Office of Science, Basic Energy Sciences (BES) (DE-SC0000957). The work at IMDEA was supported by the Spanish Ministerio de Economía y Competitividad (MINECO; Project CTQ2011-27317) and by the Campus of International Excellence (CEI) UAM+CSIC. Single crystal X-ray analysis was supported by funding from NSF Grant CHE-0840456 for X-ray instrumentation. The work at IBS was supported by Project Code (IBS-R011-D1).

DOI: 10.1021/acscentsci.5b00091
ACS Cent. Sci. 2015, 1, 94−102

REFERENCES

(1) Naito, K.; Miura, A. Molecular design for nonpolymeric organic dye glasses with thermal stability: relations between thermodynamic parameters and amorphous properties. *J. Phys. Chem.* **1993**, *97*, 6240−6248.

(2) Debenedetti, P. G.; Stillinger, F. H. Supercooled liquids and the glass transition. *Nature* **2001**, *410*, 259−267.

(3) Chen, L.; Dong, G.; Duan, L.; Wang, L.; Qiao, J.; Zhang, D.; Qiu, Y. Liquid-Formed Glassy Film of N,N′-Diphenyl-N,N′-bis(3-methylphenyl)benzidine: Formation, Carrier Transporting Ability, Photoluminescence, and Stability. *J. Phys. Chem. C* **2007**, *111*, 18376−18380.

(4) Arias, A. C.; MacKenzie, J. D.; McCulloch, I.; Rivnay, J.; Salleo, A. Materials and applications for large area electronics: solution-based approaches. *Chem. Rev.* **2010**, *110*, 3−24.

(5) Okamoto, N.; Oguni, M. Discovery of crystal nucleation proceeding much below the glass transition temperature in a supercooled liquid. *Solid State Commun.* **1996**, *99*, 53−56.

(6) Okamoto, N.; Oguni, M.; Sagawa, Y. Generation and extinction of a crystal nucleus below the glass transition temperature. *J. Phys.: Condens. Matter* **1997**, *9*, 9187−9198.

(7) Baird, J. A.; Van Eerdenbrugh, B.; Taylor, L. S. A classification system to assess the crystallization tendency of organic molecules from undercooled melts. *J. Pharm. Sci.* **2010**, *99*, 3787−3806.

(8) Whitaker, C. M.; McMahon, R. J. Synthesis and Characterization of Organic Materials with Conveniently Accessible Supercooled Liquid and Glassy Phases: Isomeric 1,3,5-Tris(naphthyl)benzenes. *J. Phys. Chem.* **1996**, *100*, 1081−1090.

(9) Greenham, N. C.; Friend, R. H. Semiconductor Device Physics of Conjugated Polymers. *Solid State Phys.* **1996**, *49*, 1−149.

(10) Veinot, J. G. C.; Marks, T. J. Toward the ideal organic light-emitting diode. The versatility and utility of interfacial tailoring by cross-linked siloxane interlayers. *Acc. Chem. Res.* **2005**, *38*, 632−643.

(11) Duan, L.; Hou, L.; Lee, T.-W.; Qiao, J.; Zhang, D.; Dong, G.; Wang, L.; Qiu, Y. Solution processable small molecules for organic light-emitting diodes. *J. Mater. Chem.* **2010**, *20*, 6392−6407.

(12) Hancock, B. C.; Parks, M. What is the True Solubility Advantage for Amorphous Pharmaceuticals? *Pharm. Res.* **2000**, *17*, 397−404.

(13) Ediger, M. D.; Angell, C. A.; Nagel, S. R. Supercooled Liquids and Glasses. *J. Phys. Chem.* **1996**, *100*, 13200−13212.

(14) Wang, L.-M.; Angell, C. A.; Richert, R. Fragility and thermodynamics in nonpolymeric glass-forming liquids. *J. Chem. Phys.* **2006**, *125*, 074505.

(15) Dounce, S. M.; Mundy, J.; Dai, H.-L. Crystallization at the glass transition in supercooled thin films of methanol. *J. Chem. Phys.* **2007**, *126*, 191111.

(16) Hecksher, T.; Nielsen, A. I.; Olsen, N. B.; Dyre, J. C. Little evidence for dynamic divergences in ultraviscous molecular liquids. *Nat. Phys.* **2008**, *4*, 737−741.

(17) Wallquist, O.; Lenz, R. 20 years of DPP pigments—future perspectives. *Macromol. Symp.* **2002**, *187*, 617−630.

(18) Li, Y.; Sonar, P.; Murphy, L.; Hong, W. High mobility diketopyrrolopyrrole (DPP)-based organic semiconductor materials for organic thin film transistors and photovoltaics. *Energy Environ. Sci.* **2013**, *6*, 1684−1710.

(19) Chandran, D.; Lee, K.-S. Diketopyrrolopyrrole: A versatile building block for organic photovoltaic materials. *Macromol. Res.* **2013**, *21*, 272−283.

(20) Ackerson, B.; Pusey, P. Shear-Induced Order in Suspensions of Hard Spheres. *Phys. Rev. Lett.* **1988**, *61*, 1033−1036.

(21) Amos, R.; Rarity, J.; Tapster, P.; Shepherd, T.; Kitson, S. Fabrication of large-area face-centered-cubic hard-sphere colloidal crystals by shear alignment. *Phys. Rev. E* **2000**, *61*, 2929−2935.

(22) Mokshin, A. V.; Barrat, J.-L. Shear-induced crystallization of an amorphous system. *Phys. Rev. E* **2008**, *77*, 021505.

(23) Karasawa, S.; Hagihara, R.; Abe, Y.; Harada, N.; Todo, J.; Koga, N. Crystal Structures, Thermal Properties, and Emission Behaviors of N, N -R-Phenyl-7-amino-2,4-trifluoromethylquinoline Derivatives: Supercooled Liquid-to-Crystal Transformation Induced by Mechanical Stimuli. *Cryst. Growth Des.* **2014**, *14*, 2468−2478.

(24) Palberg, T.; Mönch, W.; Schwarz, J.; Leiderer, P. Grain size control in polycrystalline colloidal solids. *J. Chem. Phys.* **1995**, *102*, 5082−5087.

(25) Okubo, T.; Ishiki, H. Kinetic Analyses of Colloidal Crystallization in a Wide Range of Sphere Concentrations as Studied by Reflection Spectroscopy. *J. Colloid Interface Sci.* **2000**, *228*, 151−156.

(26) Blaak, R.; Auer, S.; Frenkel, D.; Löwen, H. Crystal Nucleation of Colloidal Suspensions under Shear. *Phys. Rev. Lett.* **2004**, *93*, 068303.

(27) Grubb, D. T.; Keller, A. Crystallization induced by simple shear of molten isotactic polystyrene. *J. Polym. Sci., Polym. Lett. Ed.* **1974**, *12*, 419−425.

(28) Tribout, C.; Monasse, B.; Haudin, J. M. Experimental study of shear-induced crystallization of an impact polypropylene copolymer. *Colloid Polym. Sci.* **1996**, *274*, 197−208.

(29) Somani, R. H.; Yang, L.; Zhu, L.; Hsiao, B. S. Flow-induced shish-kebab precursor structures in entangled polymer melts. *Polymer* **2005**, *46*, 8587−8623.

(30) Sagara, Y.; Kato, T. Mechanically induced luminescence changes in molecular assemblies. *Nat. Chem.* **2009**, *1*, 605−610.

(31) Luo, X.; Li, J.; Li, C.; Heng, L.; Dong, Y. Q.; Liu, Z.; Bo, Z.; Tang, B. Z. Reversible switching of the emission of diphenyldibenzofulvenes by thermal and mechanical stimuli. *Adv. Mater.* **2011**, *23*, 3261−3265.

(32) Kwon, M. S.; Gierschner, J.; Yoon, S.-J.; Park, S. Y. Unique piezochromic fluorescence behavior of dicyanodistyrylbenzene based donor-acceptor-donor triad: mechanically controlled photo-induced electron transfer (eT) in molecular assemblies. *Adv. Mater.* **2012**, *24*, 5487−5492.

(33) Yoon, S.-J.; Chung, J. W.; Gierschner, J.; Kim, K. S.; Choi, M.-G.; Kim, D.; Park, S. Y. Multistimuli two-color luminescence switching via different slip-stacking of highly fluorescent molecular sheets. *J. Am. Chem. Soc.* **2010**, *132*, 13675−13683.

(34) Guo, Z.-H.; Jin, Z.-X.; Wang, J.-Y.; Pei, J. A donor-acceptor-donor conjugated molecule: twist intramolecular charge transfer and piezochromic luminescent properties. *Chem. Commun.* **2014**, *50*, 6088−6090.

(35) Dong, Y.; Xu, B.; Zhang, J.; Tan, X.; Wang, L.; Chen, J.; Lv, H.; Wen, S.; Li, B.; Ye, L.; Zou, B.; Tian, W. Piezochromic luminescence based on the molecular aggregation of 9,10-bis((E)-2-(pyrid-2-yl)vinyl)anthracene. *Angew. Chem., Int. Ed.* **2012**, *51*, 10782−10785.

(36) Woodall, C. H.; Brayshaw, S. K.; Schiffers, S.; Allan, D. R.; Parsons, S.; Valiente, R.; Raithby, P. R. High-pressure crystallographic and spectroscopic studies on two molecular dithienylethene switches. *CrystEngComm* **2014**, *16*, 2119−2128.

(37) The two small spikes around −25 °C in the cooling trace (one from the cooling trace to −25 °C and the other one from the cooling trace to −50 °C) might be either crack formation in DPP8 glass or electrical effect of measurement system which comes from disturbances in power supply or discharge of static electricity. Regardless of the origin, the spikes are not related to the crystallization properties of the sample because no crystallization was observed from the subsequent heating trace after cooling to −25 °C, but massive crystallization was observed from the subsequent heating trace after cooling to −50 °C.

(38) López-Mejías, V.; Kampf, J. W.; Matzger, A. J. Polymer-induced heteronucleation of tolfenamic acid: structural investigation of a pentamorph. *J. Am. Chem. Soc.* **2009**, *131*, 4554−4555.

(39) Hoffman, J. D. Thermodynamic Driving Force in Nucleation and Growth Processes. *J. Chem. Phys.* **1958**, *29*, 1192−1193.

(40) Cembran, A.; Bernardi, F.; Garavelli, M.; Gagliardi, L.; Orlandi, G. On the mechanism of the cis-trans isomerization in the lowest electronic states of azobenzene: S0, S1, and T1. *J. Am. Chem. Soc.* **2004**, *126*, 3234−3243.

(41) In the crystallization experiment of DPP12, supercooled liquid DPP12 exhibited similar shear-triggered crystallization at 85 °C

DOI: 10.1021/acscentsci.5b00091
ACS Cent. Sci. 2015, 1, 94−102

compared to DPP8. See Figure 1A for the fluorescence image of shear-triggered DPP12.
(42) Gay-Lussac, J. L. De l'influence de la pression de l'air sur la cristallisation des sels. *Ann. Chim.* **1813**, *87*, 225−236.
(43) Liu, Y.-X.; Wang, X.-J.; Lu, J.; Ching, C.-B. Influence of the roughness, topography, and physicochemical properties of chemically modified surfaces on the heterogeneous nucleation of protein crystals. *J. Phys. Chem. B* **2007**, *111*, 13971−13978.
(44) Zhang, Y.; Wang, M.; Lin, X.; Huang, W. Effect of Substrate Surface Microstructure on Heterogeneous Nucleation Behavior. *J. Mater. Sci. Technol.* **2012**, *28*, 67−72.
(45) Chrzanowska-Wodnicka, M.; Burridge, K. Rho-stimulated contractility drives the formation of stress fibers and focal adhesions. *J. Cell Biol.* **1996**, *133*, 1403−1415.
(46) Tan, J. L.; Tien, J.; Pirone, D. M.; Gray, D. S.; Bhadriraju, K.; Chen, C. S. Cells lying on a bed of microneedles: an approach to isolate mechanical force. *Proc. Natl. Acad. Sci. U.S.A.* **2003**, *100*, 1484−1489.
(47) Chen, J.; Li, H.; SundarRaj, N.; Wang, J. H.-C. Alpha-smooth muscle actin expression enhances cell traction force. *Cell Motil. Cytoskeleton* **2007**, *64*, 248−257.
(48) Reinhart-King, C. A.; Dembo, M.; Hammer, D. A. Endothelial Cell Traction Forces on RGD-Derivatized Polyacrylamide Substrate. *Langmuir* **2003**, *19*, 1573−1579.
(49) Balaban, N. Q.; Schwarz, U. S.; Riveline, D.; Goichberg, P.; Tzur, G.; Sabanay, I.; Mahalu, D.; Safran, S.; Bershadsky, A.; Addadi, L.; Geiger, B. Force and focal adhesion assembly: a close relationship studied using elastic micropatterned substrates. *Nat. Cell Biol.* **2001**, *3*, 466−472.
(50) We note that the suggested CTF of fibroblast cells may be underestimated compared to the CTF in our experimental conditions because experiments in the literature were performed on deformable substrates, and because, even within the same cell type, the exerted CTF on a substrate may increase as the substrate stiffness increases. See: Qin, L.; Genant, H. K.; Griffith, J. F.; Leung, K. S. *Advanced Bioimaging Technologies in Assessment of the Quality of Bone and Scaffold Materials*; Springer: Berlin, Heidelberg, 2007; pp 227−235.

DOI: 10.1021/acscentsci.5b00091
ACS Cent. Sci. 2015, 1, 94−102